Available online at www.sciencedirect.com
SCIENCE DIRECT®
International Journal of Thermal Sciences 44 (2005) 465–476
International Journal of Thermal Sciences
www.elsevier.com/locate/ijts

Buoyancy force and thermal radiation effects in MHD boundary layer visco-elastic fluid flow over continuously moving stretching surface

Subhas Abel [a,*], K.V. Prasad [b], Ali Mahaboob [a]

[a] *Department of Mathematics, Gulbarga University, Gulbarga, India*
[b] *Department of Mathematics, R. N. Shetty Engineering College, Bangalore, India*

Received 6 October 2003; received in revised form 25 June 2004; accepted 9 August 2004

Available online 18 November 2004

Abstract

An analysis is performed to study the effect of the Buoyancy force and thermal radiation in MHD boundary layer visco-elastic fluid flow over continuously moving stretching surface embedded in a porous medium. The following cases of surface conditions are studied namely: (i) a surface with prescribed wall temperature and (ii) a surface with prescribed heat flux. Numerical calculations have been carried out for various values of non-dimensional physical parameters, and tabulated results for Skin friction coefficient and Nusselt number, are presented and discussed.

Keywords: Visco-elastic fluid; Walters' liquid B; Grashof number; Nusselt number; Skin friction coefficient

1. Introduction

Boundary layer flow on a moving continuous surface is an important type of flow occurring in a number of engineering processes. Aerodynamic extrusion of plastic sheets, cooling of metallic sheets in a cooling bath, which would be in the form of an electrolyte, crystal growing, the boundary layer along a liquid film in condensation process and polymer sheet extruded continuously from a die are the practical applications of moving surfaces and also the materials manufactured by extrusion processes and heat treated materials travelling between a feed roll and wind up roll or on a conveyer belt possesses the characteristics of a moving continuous surfaces.

In 1961, Sakiadis [1,2] initiated the study of the boundary layer flow over a continuous solid surface moving with constant speed. Tsou et al. [3] who investigated the heat transfer effects of moving solid surface having constant velocity and temperature. In 1966, Erickson et al. [4] considered the study of heat and mass transfer in the laminar boundary layer flow of moving flat surface with constant surface velocity and temperature considering the effect of suction/injection. Soundalgekar and Ramanamurthy [5] investigated the constant surface velocity case with power law temperature variation.

There are various applications in which significant temperature differences between the body surface and the ambient fluid exist. It is usually assumed that the sheet is inextensible, but in some different situations like in the polymer industry in which it is necessary to deal with a stretching plastic sheet as mentioned by Crane [6]. Chen and Char [7] have examined the heat transfer behaviours in this flow, considering the effect of suction and injection where the boundary surface is maintained with variable temperature. Gupta and Gupta [8] have examined the similar type of problem in hydromagnetic fluid considering the uniform temperature of the boundary sheet. Considering the effect of temperature difference between the surface and ambient fluid some work have been carried out (Vajravelu and Rollins [9], Vajravelu and Nayfeh [10]) on the flow and heat transfer introducing temperature dependent heat source/sink.

* Corresponding author.
E-mail address: msabel2001@yahoo.co.uk (S. Abel).

1290-0729/$ – see front matter
doi:10.1016/j.ijthermalsci.2004.08.005

Nomenclature

x, y	distance along and perpendicular to the surface, respectively
u, v	components of velocities along and perpendicular to the surface, respectively
k_1	visco-elastic parameter
k_2	permeability parameter
B_0	magnetic induction
C_p	specific heat at constant pressure
g	acceleration due to gravity
K	thermal conductivity
Mn	magnetic field parameter
Nu	Nusselt number
Pr	Prandtl number
Gr	Grashof number
T	temperature

Greek symbols

η	dimensionless normal distance
θ	dimensionless temperature
α	heat source/sink parameter
σ	fluid electrical conductivity
ρ	fluid density
γ	fluid kinematic viscosity
μ	fluid dynamic viscosity
τ	Skin friction coefficient

There are several practical applications in which significant temperature differences between the surface of the body and the ambient fluid exist. The temperature differences cause density gradients in the fluid medium, and in presence of gravitational force, free convection effects become more important. A situation where both the forced and free convection are of comparable order is called mixed convection. Brown [11] studied the effect of the coefficient of volumetric expansion on laminar free convection heat transfer. Various relations between the physical properties of fluids and temperature are given by Kays [12]. Grubka and Bobba [13] analysed the stretching problem for surface moving with linear velocity and with variable surface temperature. Temperature distribution in the steady plane flow of a viscous fluid towards a stretching surface was investigated by Ray Mahapatra and Gupta [14].

All the above analyses are restricted to the flow of Newtonian fluids. However, in reality, most of liquids used in industrial applications particularly in polymer processing applications are of non-Newtonian in nature. In view of this, the study of above boundary layer flow problem has been further channelised to the non-Newtonian fluid flow. Considering the survey of literature it is noticed that Rajgopal et al. [15] considered the study of visco-elastic second order fluid flow over a stretching sheet by solving the boundary layer equation numerically. Siddappa and Abel [16] have presented a similar flow analysis without heat transfer in the flow of non-Newtonian fluid of the type

Walters' liquid B. Exact analytical solutions of MHD flow of a visco-elastic Walters' liquid B past a stretching sheet has been presented by Anderson [17]. The effects of internal heat generation on heat transfer phenomena are excluded from their analysis. In non-Newtonian fluid flow, like the one of the Walters' liquid B, the effect of frictional heating plays a significant role in heat transfer processes.

The non-Newtonian fluids are being considered more important and appropriate in technological applications in comparison with Newtonian fluids. A large class of real fluids does not exhibit the linear relationship between stress and rate of strain. Because of non-linear dependence, the analysis and behaviour of non-Newtonian fluids tends to be much more complicated and subtle in comparison to Newtonian fluids. In the literature there is fairly large number of flows of Newtonian fluids for which a closed form analytical solution is possible.

However, all these researchers restrict their analysis to hydromagnetic flow and heat transfer. None of them deals with much more intricate problem involving the effect of thermal radiation on hydromagnetic visco-elastic fluid flow. Perdikis and Raptis [18], Raptis and Perdikis [19], Raptis [20] and Ckamka [21], which shows that the work is not carried out for visco-elastic fluids of the type Walters' liquid B where the thermal conductivity is a function of temperature.

Keeping this in view, in the present paper, we contemplate to study the Buoyancy effect as well as the effect of variable thermal conductivity on thermal radiation of hydromagnetic flow of a visco-elastic fluid over a moving stretching surface.

2. Mathematical formulation

Consider a steady, laminar free convective flow of an incompressible and electrically conducting visco-elastic fluid over continuously moving stretching surface embedded in a porous medium. Two equal and opposite forces are introduced along x-axis so that sheet is stretched with a speed proportional to the distance from the origin. The resulting motion of the otherwise quiescent fluid is thus caused solely by the moving surface. A uniform magnetic field of strength B_0 is imposed along y-axis. This flow satisfies the rheological equation of state derived by Beard and Walters in 1964.

The steady two-dimensional boundary layer equations in usual notation are,

$$\frac{\partial u}{\partial x} + \frac{\partial v}{\partial y} = 0 \tag{1}$$

$$u\frac{\partial u}{\partial x}+v\frac{\partial u}{\partial y}=\gamma\frac{\partial^2 u}{\partial y^2}-k_o\left\{u\frac{\partial^3 u}{\partial x\partial y^2}+v\frac{\partial^3 u}{\partial y^3}+\frac{\partial u}{\partial x}\frac{\partial^2 u}{\partial y^2}-\frac{\partial u}{\partial y}\frac{\partial^2 u}{\partial x\partial y}\right\}-\frac{\sigma B_o^2 u}{\rho}-\frac{\gamma}{k'}u+g\beta\,(T-T_\infty) \tag{2}$$

Here x and y are respectively the directions along and perpendicular to the surface, u, v are the velocity components along x and y directions, respectively, and other symbols have their usual meanings. The last term in Eq. (2) leads to the Buoyancy force.

In deriving these equations, it is assumed, in addition to the usual boundary layer approximations that the contribution due to the normal stress is of the same order of magnitude as the shear stress.

The boundary conditions applicable to the flow problem are,

$$\begin{aligned} &u=bx, && v=0 && \text{at } y=0\\ &u\to 0, && u_y\to 0 && \text{as } y\to\infty \end{aligned} \tag{3}$$

Eqs. (1) and (2) admit self-similar solution of the form,

$$u=bxf_\eta(\eta),\qquad v=-\sqrt{b\gamma}\,f(\eta),\qquad \text{where } \eta=\sqrt{\frac{b}{\gamma}}y \tag{4}$$

where subscript η denotes the derivative with respect to η. Clearly u & v satisfy Eq. (1) identically. Substituting these new variables in Eq. (2), we have,

$$f_\eta^2-ff_{\eta\eta}=f_{\eta\eta\eta}-k_1\{2f_\eta f_{\eta\eta\eta}-ff_{\eta\eta\eta\eta}-f_{\eta\eta}^2\}-Mn\,f_\eta-k_2 f_\eta+Gr\,\theta \tag{5}$$

where

$$k_1=\frac{k_0 b}{\gamma},\qquad k_2=\frac{\gamma}{bk'}$$

$$Mn=\frac{\sigma B_0^2}{b\rho},\qquad Gr=\frac{g\beta A}{b^2 l}$$

Similarly boundary conditions (3) takes the form

$$\begin{aligned} &f_\eta(\eta)=1, && f(\eta)=0 && \text{at } \eta=0\\ &f_\eta(\eta)\to 0, && f_{\eta\eta}(\eta)\to 0 && \text{as } \eta\to\infty \end{aligned} \tag{6}$$

3. Heat transfer analysis

The energy equation in the presence of radiation and internal heat generation/absorption for two-dimensional flow is

$$u\frac{\partial T}{\partial x}+v\frac{\partial T}{\partial y}=\frac{1}{\rho C_p}\frac{\partial}{\partial y}\left(K\frac{\partial T}{\partial y}\right)+\frac{Q}{\rho C_p}(T-T_\infty)-\frac{1}{\rho C_p}\frac{\partial q_r}{\partial y} \tag{7}$$

The thermal conductivity K is assumed to vary linearly with temperature and it is of the form:

$$K=K_\infty\big(1+\varepsilon\theta(\eta)\big) \tag{8}$$

where

$$\theta(\eta)=\frac{T-T_\infty}{T_w-T_\infty}\quad\text{and}\quad\varepsilon=\frac{K_w-K_\infty}{K_\infty}$$

is a small parameter.

By using Rosseland approximation (Brewster in 1992) the radiative heat flux is given by

$$q_r=-\frac{4\sigma^*}{3K^*}\frac{\partial T^4}{\partial y} \tag{9}$$

where σ^* and K^* are respectively the Stephan–Boltzman constant and the mean absorption coefficient. We assume the differences within the flow are such that T^4 can be expressed as a linear function of temperature. Expanding T^4 in a Taylor series about T_∞ and neglecting higher order terms thus,

$$T^4\cong 4T_\infty^3 T-3T_\infty^4 \tag{10}$$

The boundary conditions are

$$\begin{aligned} &T=T_w=T_\infty+A\left(\frac{x}{l}\right) && \text{at } y=0 && \text{PST case}\\ &-KT_y=Q_w=D\left(\frac{x}{l}\right) && \text{at } y=0 && \text{PHF case}\\ &T\to T_\infty && \text{as } y\to\infty \end{aligned} \tag{11}$$

Now using Eqs. (8)–(10), Eq. (7) becomes

$$\big(1+\varepsilon\theta(\eta)+Nr\big)\theta_{\eta\eta}(\eta)+Pr\,f(\eta)\theta_\eta(\eta)-Pr\big(f_\eta(\eta)-\alpha\big)\theta(\eta)+\varepsilon\theta_\eta^2=0 \tag{12}$$

where

$$Pr=\frac{\mu C_p}{K_\infty},\qquad Nr=\frac{16\sigma^* T_\infty^3}{3K^*K_\infty},\qquad \alpha=\frac{Q}{b\rho C_p}$$

The boundary conditions (11) takes the form:

$$\begin{aligned} &\theta(0)=1, && \theta(\eta)\to 0 && \text{as } \eta\to\infty && \text{PST case}\\ &\theta_\eta(0)=-1, && \theta(\eta)\to 0 && \text{as } \eta\to\infty && \text{PHF case} \end{aligned} \tag{13}$$

Our interest lies in investigation of the flow behaviour and heat transfer characteristics by analyzing the non-dimensional local shear stress (τ_w) and Nusselt number (Nu). These non-dimensional parameters are defined as:

$$\tau_w=\frac{\tau^*}{\mu bx\sqrt{b/\gamma}}=f_{\eta\eta}(0),\quad\text{where } \tau^*=-\mu\left(\frac{\partial u}{\partial y}\right)_{y=0}$$

$$Nu=\frac{-h}{T_w-T_\infty}T_y=\begin{cases}\theta_\eta(0) & \text{PST case}\\ 1/\theta(0) & \text{PHF case}\end{cases} \tag{14}$$

4. Method of solution

Because of the momentum and the thermal boundary layer equations being nonlinear and coupled, exact solutions do not seem feasible for complete set of Eqs. (5), (6),

(12) and (13) and therefore solution must be obtained numerically. In order to solve them, we employ most efficient shooting technique with fourth order Runge–Kutta integration scheme, which is described in Abel et al. [22].

Selection of an appropriate finite value of η_∞ is most important aspect in this method. To select η_∞, we begin with some initial guess value and solve the problem with some particular set of parameters to obtain $f_{\eta\eta}(0)$ and $\theta_k(0)$ ($\theta_k = \theta_\eta$ in PST case and $\theta_k = \theta$ in PHF case). The solution process is repeated with another larger (or smaller, as the case may be) value of η_∞. The values of $f_{\eta\eta}(0)$ and $\theta_k(0)$ compared to their respective previous values, if they agreed to about six significant digits, the last value of η_∞ used was considered the appropriate value for that particular set of parameters; otherwise the procedure was repeated until further changes in η_∞ which did not lead to any more change in the values of $f_{\eta\eta}(0)$ and $\theta_k(0)$. The initial step size employed was $h = 0.01$. The convergence criterion largely depends on fairly good guesses of the initial conditions in the shooting technique (Chiam [23]), and is based on the relative difference between the current and the previous iterations used, when this difference reaches 10^{-5} the solution is assumed to have converged and the iterative process is terminated.

Eqs. (5) and (13) constitute a highly nonlinear coupled boundary value problem of fourth order in f and second order in θ respectively, has been reduced to a system of six simultaneous coupled ordinary differential equations by assuming $f = f_1$, $f_\eta = f_2$, $f_{\eta\eta} = f_3$, $f_{\eta\eta\eta} = f_4$, $\theta = \theta_1$, and $\theta_\eta = \theta_2$. In order to solve this resultant system, we need to have six initial conditions, whilst we have only two initial conditions on f and one initial condition on θ. The third initial condition on f (i.e., $f_4(0)$) is obtained in terms of physical parameters by applying the initial conditions of (6) and (13) (Lawrence and Rao, 1995). Since $f_3(0)$ and $\theta_k(0)$ ($k = 2$ in PST case & $k = 1$ in PHF case) which are not prescribed, we start with the initial approximations as $f_3(0) = \alpha_0$ and $\theta_k(0) = \beta_0$. Let α and β be the correct values of $f_3(0)$ and $\theta_k(0)$, respectively. Now we integrate the resultant system of six ordinary differential equations using standard fourth order Runge–Kutta method and denote the values of f_3 and θ_k at $\eta = \eta_\infty$ by $f_3(\alpha_0, \beta_0, \eta_\infty)$ and $\theta_k(\alpha_0, \beta_0, \eta_\infty)$, respectively. Since f_3 & θ_k at $\eta = \eta_\infty$ are clearly functions of α and β, they are expanded in Taylor series around $\alpha - \alpha_0$ and $\beta - \beta_0$, respectively, retaining only the linear terms. We use the difference quotients for the derivatives appeared in these Taylor series expansions. Now, after solving the system of Taylor series expansions for $\delta\alpha_0 = \alpha - \alpha_0$ and $\delta\beta_0 = \beta - \beta_0$, we obtain the new estimates $\alpha_1 = \alpha_0 + \delta\alpha_0$ and $\beta_1 = \beta_0 + \delta\beta_0$. The entire process is repeated starting with $f_1(0), f_2(0), \alpha_1, f_4(0), \theta_1(0)$ and β_1 as initial conditions. Iteration of the whole outline procedure is continued with the latest estimates of α and β, until we obtain the computed values of prescribed boundary conditions. Finally, we obtain $\alpha_n = \alpha_{n-1} + \delta\alpha_{n-1}$, $\beta_n = \beta_{n-1} + \delta\beta_{n-1}$ for $n = 1, 2, 3, \ldots$ as the desired most approximate initial values of $f_3(0)$ and $\theta_k(0)$. With this now all the six initial conditions become known and so we solve the resultant system of six simultaneous equations by fourth order Runge–Kutta integration scheme and get the profiles of f_1, f_2, f_3, f_4, θ_1 and θ_2 for a particular set of parameters.

5. Results and discussion

In order to test the accuracy of our present method, we have compared our results with that of previous works in the absence of thermal radiation and Buoyancy effects, which are found to be excellent in agreement. For different values of physical parameters, numerical values of horizontal velocity profile $f_\eta(\eta)$ are illustrated in Figs. 1–4 and numerical values of temperature profile $\theta(\eta)$ for both Prescribed Surface Temperature (PST Case) and Prescribed Heat Flux (PHF Case) are illustrated in Figs. 5–10.

The effect of visco-elastic parameter and porosity parameter on the horizontal velocity profile in the boundary layer is shown in Fig. 1. It is observed that velocity decreases in the boundary layer with the increase of distance from the boundary. The effect of visco-elastic parameter is to decrease the velocity in the boundary. This result is consistent with the fact that the introduction of tensile stress due to visco-elasticity cause transverse contraction of the boundary layer and hence velocity decreases. This behaviour is even true in presence of porous medium.

Fig. 2 illustrates that the effect of magnetic parameter, i.e., the introduction of transverse magnetic field normal to the flow direction have a tendency to create a drag due to Lorentz force which tends to resist the flow and, hence the horizontal velocity boundary layer decreases. This result is even true for the presence of porous media (k_2) and heat source/sink parameter (α).

The effect of thermal radiation parameter (Nr) on horizontal velocity profile in the presence/absence of magnetic parameter (Mn) and also of porous parameter is shown in Fig. 3. It is noticed that effect of thermal radiation parameter, is to enhance velocity in the boundary layer. From Fig. 4 it is observed that horizontal velocity profile increases with the increase of Grashof number (Gr). This demonstrates the role of convection current as to increase the horizontal velocity component. This result is even true for the presence of porosity parameter. In this case, there is velocity overshoot (i.e., the velocity at a certain value of η exceeds the velocity at the edge of the boundary layer) in the boundary layer region and Buoyancy force act like a favourable pressure gradient and accelerates the fluid within the boundary layer which is similar to the result obtained by Takhar et al. [24] for viscous flows.

The effect of Magnetic parameter on temperature profile for both PST and PHF cases in presence/absence of porosity parameter and heat source/sink parameter is shown in Figs. 5 and 6, respectively. It is observed that the effect of magnetic parameter is to increase the temperature profile in the boundary layer. The Lorentz force has the tendency to slow down

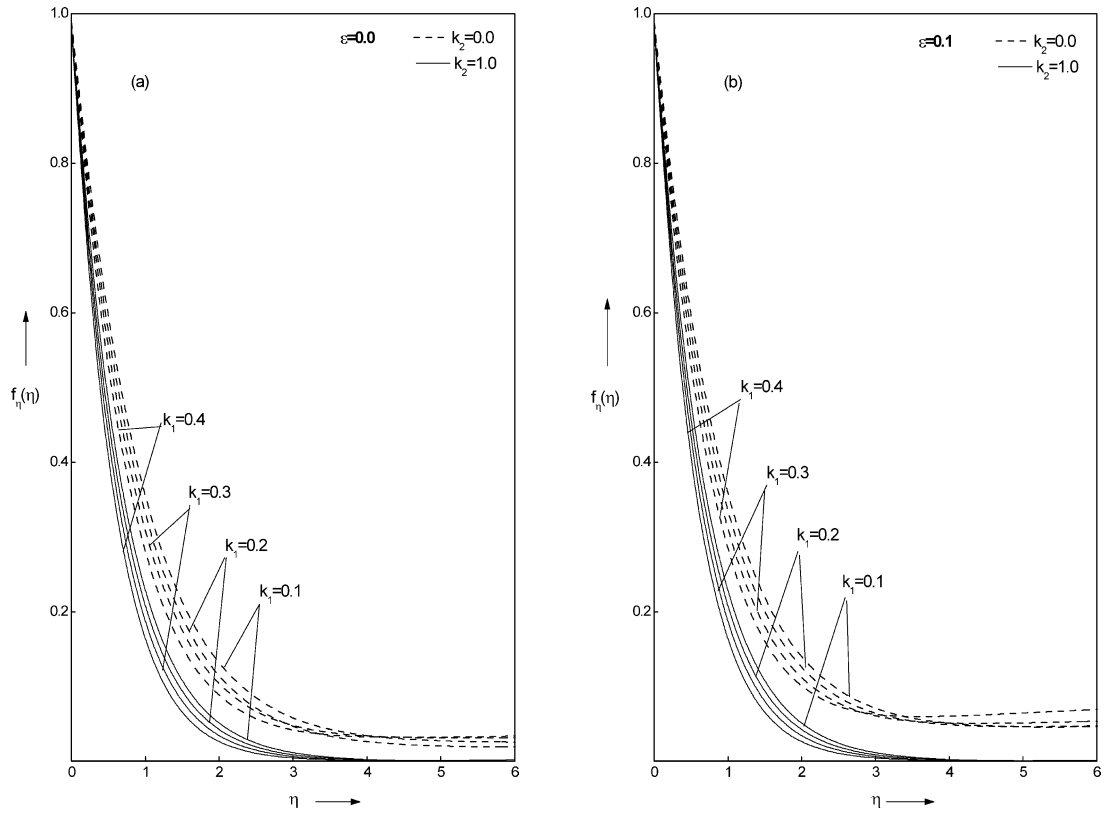

Fig. 1. Variation of $f_\eta(\eta)$ vs. η for different values of visco-elastic parameter k_1, porosity parameter k_2 and thermal conductivity parameter ε when $Pr = 1.0$, $Mn = 0.0$, $\alpha = 0.0$, $Nr = 0.0$, and $Gr = 0.0$.

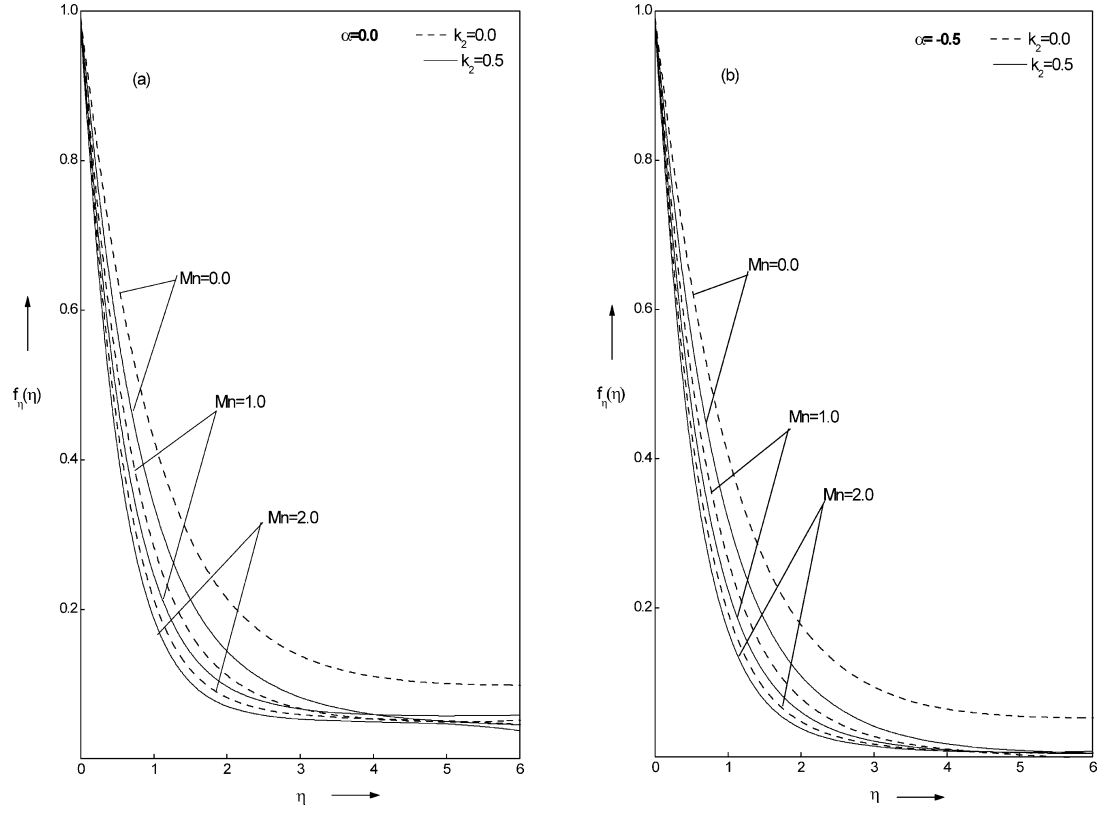

Fig. 2. Variation of $f_\eta(\eta)$ vs. η for different values of magnetic parameter Mn, porosity parameter k_2 and heat source/sink parameter α when $Pr = 1.0$, $k_1 = 0.1$, $\varepsilon = 0.1$, $Nr = 1.0$, and $Gr = 0.2$.

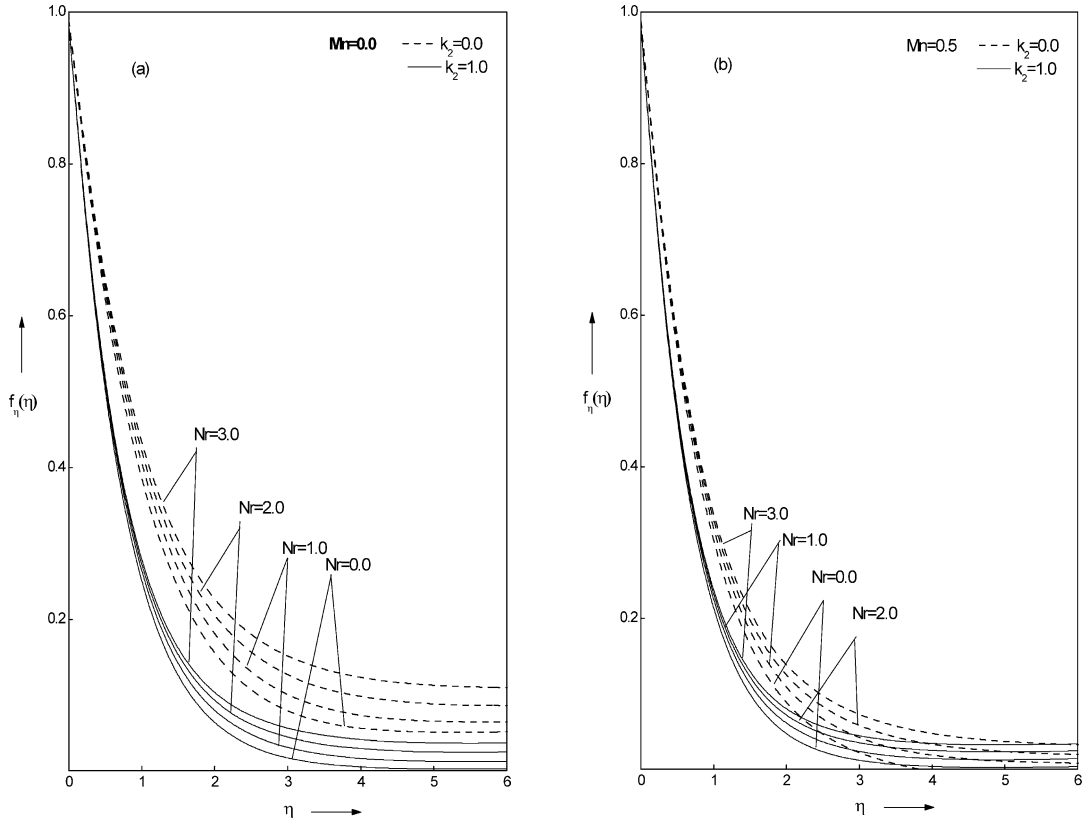

Fig. 3. Variation of $f_\eta(\eta)$ vs. η for different values of thermal radiation parameter Nr, magnetic parameter Mn and porosity parameter k_2 when $Pr = 1.0$, $k_1 = 0.1$, $Gr = 0.2$, $\alpha = 0.5$, and $\varepsilon = 0.0$.

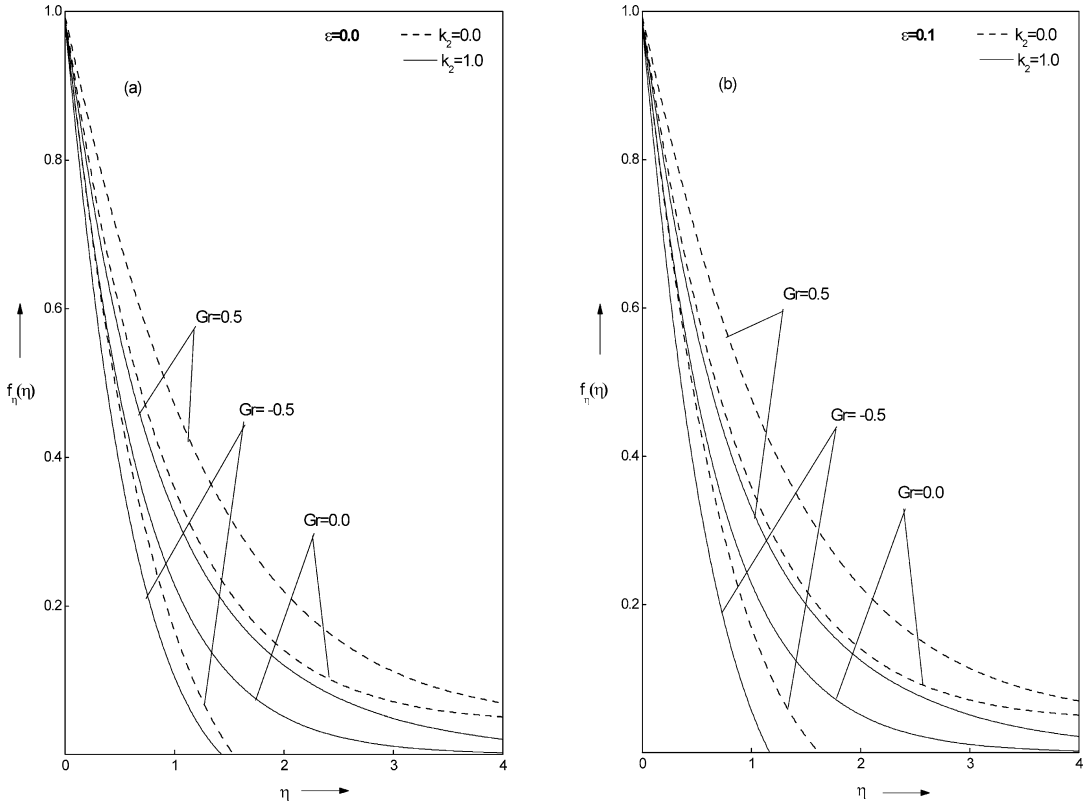

Fig. 4. Variation of $f_\eta(\eta)$ vs. η for different values of Grashof number Gr, porosity parameter k_2 and thermal conductivity parameter ε when $Pr = 1.0$, $Mn = 0.0$, $\alpha = 0.5$, $Nr = 1.0$, and $k_1 = 0.1$.

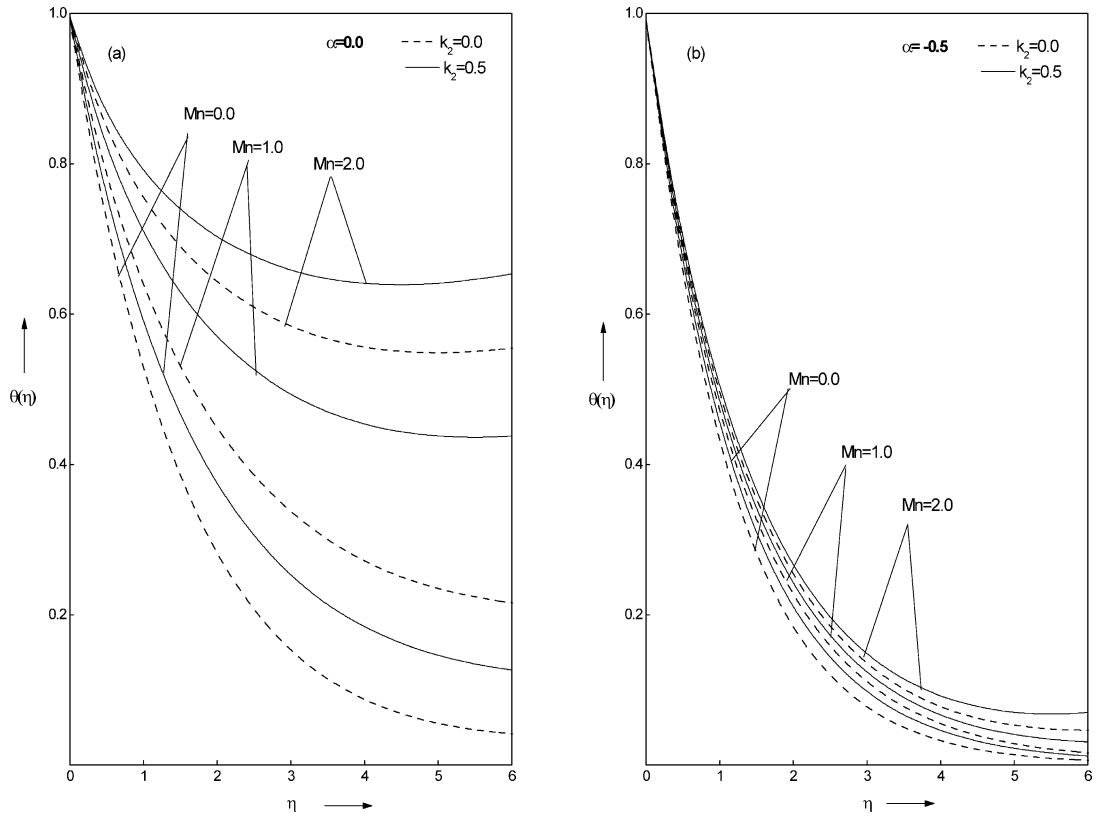

Fig. 5. Variation of $\theta(\eta)$ vs. η for different values of magnetic parameter Mn, porosity parameter k_2 and heat source/sink parameter α when $Pr = 1.0$, $k_1 = 0.1$, $\varepsilon = 0.1$, $Nr = 0.0$, and $Gr = 0.2$ in PST case.

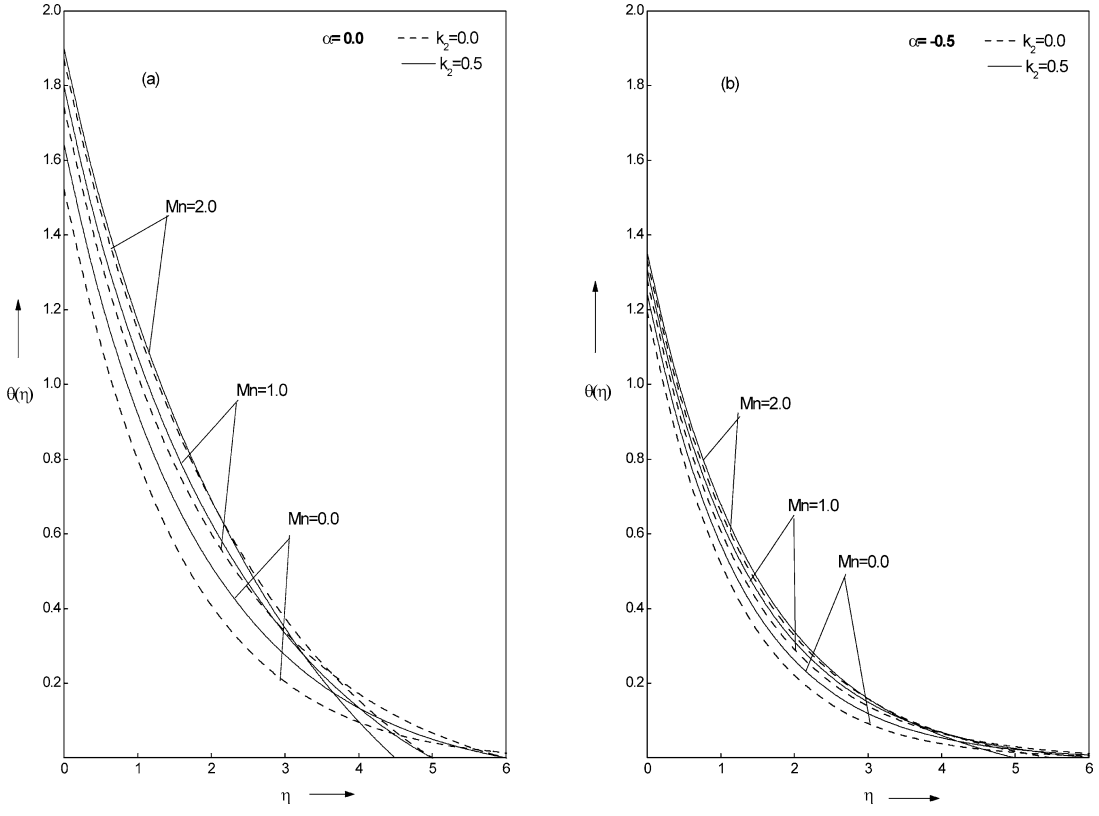

Fig. 6. Variation of $\theta(\eta)$ vs. η for different values of magnetic parameter Mn, porosity parameter k_2 and heat source/sink parameter α when $Pr = 1.0$, $k_1 = 0.1$, $\varepsilon = 0.1$, $Nr = 0.0$, and $Gr = 0.2$ in PHF case.

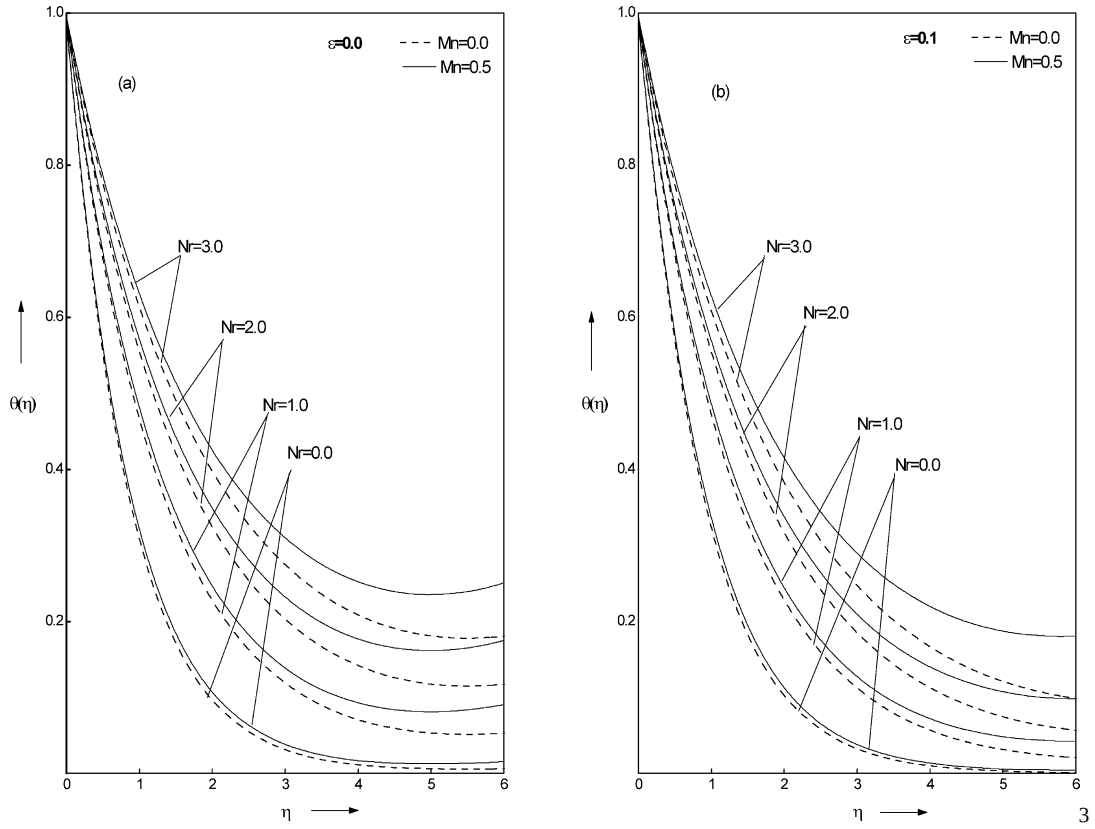

Fig. 7. Variation of $\theta(\eta)$ vs. η for different values of thermal radiation parameter Nr, magnetic parameter Mn and thermal conductivity parameter ε when $Pr = 1.0$, $k_1 = 0.1$, $Gr = 0.2$, $\alpha = 0.5$, and $k_2 = 1.0$ in PST case.

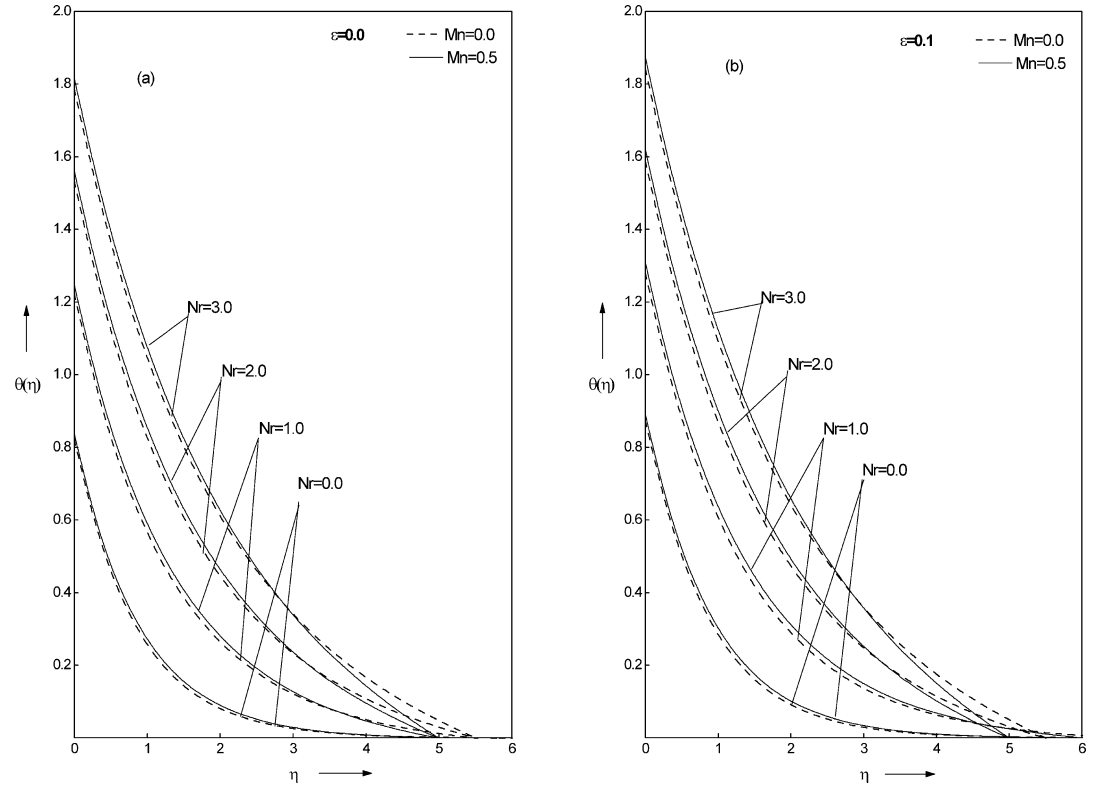

Fig. 8. Variation of $\theta(\eta)$ vs. η for different values of thermal radiation parameter Nr, magnetic parameter Mn and thermal conductivity parameter ε when $Pr = 1.0$, $k_1 = 0.1$, $k_2 = 1.0$, $\alpha = 0.5$, and $Gr = 0.2$ in PHF case.

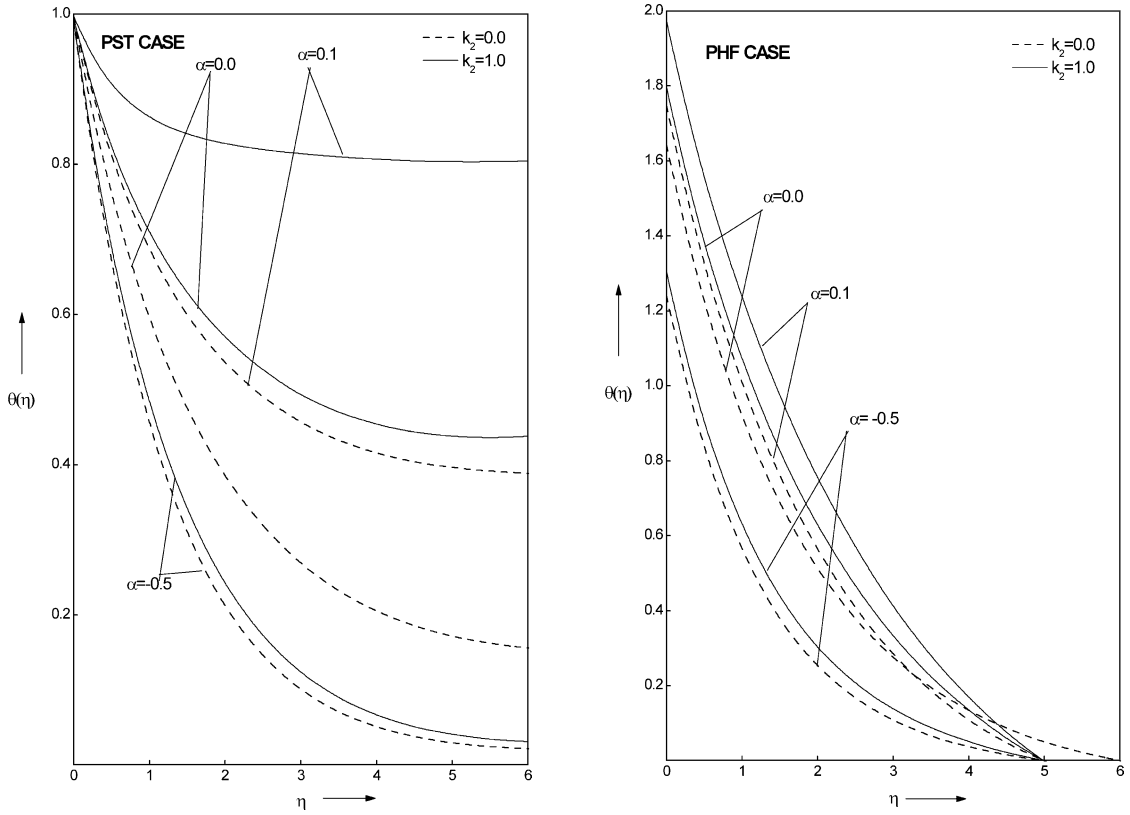

Fig. 9. Variation of $\theta(\eta)$ vs. η for different values of heat source/sink parameter α, porosity parameter k_2 and Grashof number Gr when $Pr = 1.0$, $k_1 = 0.1$, $Mn = 0.5$, $Nr = 1.0$, and $\varepsilon = 0.1$.

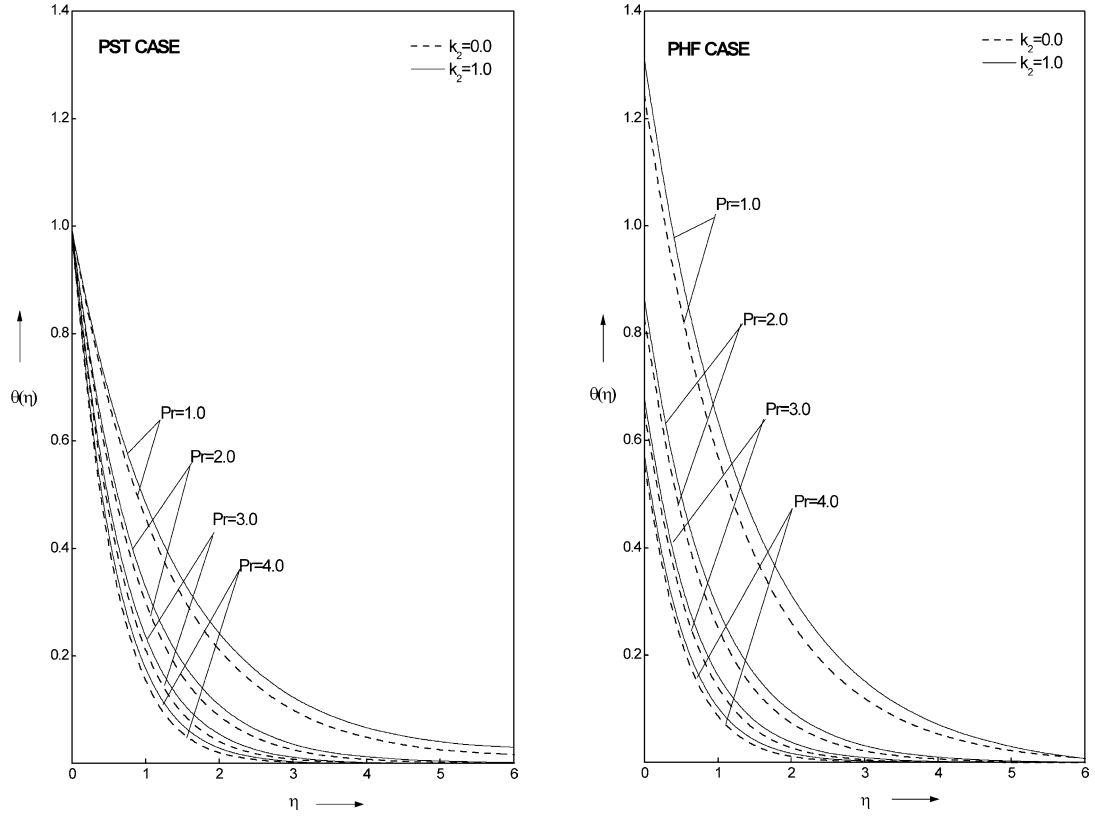

Fig. 10. Variation of $\theta(\eta)$ vs. η for different values of Prandtl number Pr and porosity parameter k_2 when $k_1 = 0.1$, $Mn = 0.5$, $Nr = 1.0$, $\alpha = 0.5$, and $Gr = 0.2$.

Table 1
Values of Skin friction coefficient and Heat transfer coefficient for different values of non-dimensional physical parameters in PST case

k_1	k_2	Pr	Mn	α	Gr	Nr	ε	PST case	
								$f_{\eta\eta}(0)$	$\theta_\eta(0)$
0.1	0.0	1.0	0.0	−0.5	0.5	1.0	0.0	−0.73017700	−0.87268680
					0.0			−1.06515444	−0.84444766
					−0.5			−1.42888733	−0.63990226
	1.0				0.5			−1.27583186	−0.82389936
					0.0			−1.52855339	−0.79039331
					0.5			−1.82960981	−0.67630871
	0.0				0.5		0.1	−0.72122243	−0.84044242
					0.0			−1.06515444	−0.81561844
					−0.5			−1.43617297	−0.61082164
	1.0				0.5			−1.27364622	−0.79617087
					0.0			−1.52855192	−0.76297405
					−0.5			−1.80395270	−0.71534442
0.1	1.0	1.0	0.5	−0.5	0.2	0.0	0.0	−1.63318940	−1.17935033
						1.0		−1.61918692	−0.78130683
						2.0		−1.61125621	−0.60723765
						3.0		−1.06587194	−0.50393283
						0.0	0.1	−1.63171020	−1.10289975
						1.0		−1.61891582	−0.75837478
						2.0		−1.61167500	−0.60049479
						3.0		−1.60673269	−0.50171570
0.1	0.0	1.0	0.5	0.2	0.2	1.0	0.0	−1.15764074	−0.40863490
				0.0				−1.18520669	−0.59182635
				−0.5				−1.20744748	−0.82780966
				0.2			0.1	−1.20381049	−0.56637338
				0.0				−1.18403381	−0.57061521
				−0.5				−1.20596476	−0.79915255
0.1	1.0	1.0	0.5	−0.5	0.2	1.0	0.0	−1.61918692	−0.78130683
		2.0						−1.63318940	−1.17935033
		3.0						−1.64134846	−1.49009886
		4.0						−1.64709652	−1.75542170
		1.0					0.1	−1.61891582	−0.75837478
		2.0						−1.63250413	−1.13991460
		3.0						−1.64066945	−1.44016386
		4.0						−1.64642999	−1.69659872

the motion of the fluid in the boundary layer and to increase its temperature profile. Also the effect on the flow and thermal fields become more so as the strength of the magnetic field increases. The effect of magnetic parameter is to increase the wall temperature gradient in PST case and Wall temperature in PHF case.

Figs. 7 and 8 illustrate the effect of thermal radiation on temperature profile in the boundary layer for both PST and PHF cases, respectively. It is observed that the increase in thermal radiation parameter produces a significant increase in the thickness of the thermal boundary layer of the fluid and so as the temperature profile increases in presence/absence of thermal conductivity parameter (ε).

The effect of heat source/sink parameter on temperature profile in the boundary layer for both PST and PHF cases is shown in Fig. 9(a) and (b), respectively. The direction of heat flow depends both on temperature difference $(T_w - T_\infty)$ and the temperature gradient $\theta_\eta(0)$. However in the heat sources, Q and $(T_w - T_\infty)$ have the same sign since $-\theta_\eta(0)$ is positive. To interpret the heat transfer result physically, we discuss the result of positive α and negative α separately. For positive α, we have a heat source in the boundary layer when $T_w < T_\infty$ and heat sink when $T_w > T_\infty$. Physically, these correspond, respectively, recombination and dissociation within the boundary layer. For the case of cooled wall ($T_w < T_\infty$), there is heat transfer from the fluid to the wall even without heat source. The presence of heat source ($\alpha > 0$) will further increase the heat flow to the wall.

When α is negative, this indicates a heat source for $T_w > T_\infty$ and a heat sink for $T_w < T_\infty$. This corresponds to com-

Table 2
Values of Skin friction coefficient and Heat transfer coefficient for different values of non-dimensional physical parameters in PHF case

k_1	k_2	Pr	Mn	α	Gr	Nr	ε	PST case	
								$f_{\eta\eta}(0)$	$\theta_\eta(0)$
0.1	0.0	1.0	0.0	−0.5	0.5	1.0	0.0	−0.73873634	1.13027391
					0.0			−1.06515444	1.18321148
					−0.5			−1.47604730	1.21985682
	1.0				0.5			−1.22654534	1.20342956
					0.0			−1.52855338	1.26305452
					0.5			−1.87352301	1.30885021
	0.0				0.5		0.1	−0.72277264	1.17372434
					0.0			−1.06515444	1.23467515
					−0.5			−1.49131624	1.28940562
	1.0				0.5			−1.21097982	1.25337939
					0.0			−1.52855192	1.32279955
					−0.5			−1.94641306	1.47396730
0.1	1.0	1.0	0.5	−0.5	0.2	0.0	0.0	−1.64586137	0.84824379
						1.0		−1.59581870	1.25912242
						2.0		−1.55604548	1.57267369
						3.0		−1.52326262	1.82714364
						0.0	0.1	−1.64014616	0.90162562
						1.0		−1.58836540	1.32024605
						2.0		−1.54891640	1.63080015
						3.0		−1.51605757	1.88470677
0.1	0.0	1.0	0.5	0.1	0.2	1.0	0.1	−1.09717466	1.75949365
				0.0				−1.11345074	1.65380302
				−0.5				−1.17905916	1.25083432
	1.0			0.1				−1.50127773	1.98569943
				0.0				−1.52473038	1.80881940
				−0.5				−1.58836540	1.32024605
0.1	1.0	1.0	0.5	−0.5	0.2	1.0	0.0	−1.59581870	1.25912242
		2.0						−1.64586137	0.84824379
		3.0						−1.66584644	0.67230399
		4.0						−1.67670242	0.57085834
		1.0					0.1	−1.58836540	1.32024605
		2.0						−1.64305722	0.87448201
		3.0						−1.66430361	0.68862489
		4.0						−1.67565412	0.58251981

bustion and an endothermic chemical reaction. For the case of heated wall ($T_w > T_\infty$), the presence of a heat source ($\alpha < 0$) creates a layer of hot fluid adjacent to the surface and therefore the heat from the wall decreases. For cooled wall case ($T_w < T_\infty$), the presence of heat sink ($\alpha < 0$) blankets the surface with a layer of cool fluid, and therefore heat flow into the surface decreases. This result is similar to the result obtained by Acharya et al. [25].

Fig. 10(a) and (b) illustrate the effect of Prandtl number (Pr) on temperature profile in the boundary for both PST and PHF cases, respectively. It is observed that the effect of Prandtl number is to decrease the temperature profile in the boundary layer.

The values of Skin friction coefficient $f_{\eta\eta}(0)$ and Nusselt number Nu, for various values of non-dimensional physical parameters are recorded in Tables 1 and 2 for both PST and PHF cases, respectively. It was found that the skin friction coefficient increased due to increase in the heat absorption coefficient, and the effect of Grashof number is to decrease the Nusselt number in both cases and is even true in presence of porous medium.

6. Conclusion

The governing equations for a steady, laminar free convective flow of an incompressible and electrically conducting visco-elastic fluid over continuously moving stretching surface embedded in a porous medium was formulated. The resulting partial differential equations are transformed into ordinary differential equations by using similarity transformations. Numerical evaluations were performed and graphical results were obtained to illustrate the details of flow and heat transfer characteristics and their dependence on some

of the physical parameters. It was found that when Grashof number increased, the fluid velocity increased. However it is observed that the effect of heat source in the boundary layer generates energy, which causes the temperature to increase, while the presence of heat absorption effects caused reductions in the fluid temperature, which results in decreasing the fluid velocity. It is also observed that increase in thermal radiation parameter produces a significant increase in the thickness of the thermal boundary layer of the fluid and so as the temperature increases in presence/absence of thermal conductivity parameter. Analysis of the tables shows that the magnitude of surface velocity gradient is found to increase with the viscoelastic parameter k_1, in the absence of Buoyancy force and the effect of Grashof number is to decrease the Nusselt number in both cases and is even true in presence of porous medium.

References

[1] B.C. Sakiadis, Boundary layer behaviour on continuous solid surfaces: I Boundary layer equations for two dimensional and axisymmetric flow, AIChE. J. 7 (1961) 26–28.
[2] B.C. Sakiadis, Boundary layer behaviour on continuous solid surfaces: II Boundary layer on a continuous flat surface, AIChE. J. 7 (1961) 221–225.
[3] F.K. Tsou, F.K. Sparrow, R.J. Goldstein, Flow and heat transfer in the boundary layer on a continuous moving surface, Internat. J. Heat Mass Transfer 10 (1967) 219–223.
[4] L.E. Erickson, L.T. Fan, V.G. Fox, Heat and Mass transfer on a moving continuous flat plate with suction or injection, Indust. Engrg. Chem. Fund 5 (1966) 19–25.
[5] V.M. Soundalgekar, T.V. Ramanamurthy, Heat transfer in the flow past a continuous moving plate with variable temperature, Warme und Stoffubertragung 14 (1980) 91–93.
[6] L.J. Crane, Flow past a stretching plate, Z. Angew. Math. Phys. 21 (1970) 645–647.
[7] C.K. Chen, M.I. Char, Heat transfer of a continuous stretching surface with suction or blowing, J. Math. Anal. Appl. 135 (1988) 568–580.
[8] P.S. Gupta, A.S. Gupta, Heat and Mass transfer on a stretching sheet with suction or blowing, Canad. J. Chem. Engrg. 55 (1977) 744–746.
[9] K. Vajravelu, D. Rollins, Heat transfer in electrically conducting fluid over a stretching surface, Internat. J. Non-Linear Mech. 27 (2) (1992) 265–277.
[10] K. Vajravelu, J. Nayfeh, Convective heat transfer at a stretching sheet, Acta. Mech. 96 (1993) 47–54.
[11] A. Brown, Trans. ASME. Ser. C. J. Heat Transfer 97 (1975) 133–135.
[12] W.M. Kays, M.E. Grawford, Convection Heat and Mass Transfer, Pergamon, Oxford, 1980.
[13] L.J. Grubka, K.M. Bobba, Heat transfer characteristics of a continuous stretching surface with variable temperature, ASME J. Heat Transfer 107 (1985) 248–250.
[14] T. Ray Mahapatra, A.S. Gupta, Heat Transfer in stagnation point flow towards a stretching sheet, Heat Mass Transfer 38 (2002) 517.
[15] K.R. Rajgopal, T.Y. Na, A.S. Gupta, Flow of visco-elastic fluid over a stretching sheet, Rheol. Acta 23 (1984) 213–215.
[16] B. Siddappa, S. Abel, Non-Newtonian flow past a stretching plate, Z. Angew. Math. Phys. 36 (1985) 890–892.
[17] H.I. Andersson, MHD flow of a visco-elastic fluid past a stretching surface, Acta Mech. 95 (1992) 227–230.
[18] C. Perdikis, A. Raptis, Heat transfer of a micro-polar fluid by the presence radiation, Heat Mass Transfer 31 (1996) 381–382.
[19] A. Raptis, C. Perdikis, Visco-elastic flow by the presence of radiation, Z. Angew. Math. Mech. 78 (1998) 277–279.
[20] A. Raptis, Radiation and visco-elastic flow, Internat. Comm. Heat Mass Transfer 26 (1999) 889–895.
[21] A.J. Ckamka, Thermal radiation and Bouyancy effects on hydromagnetic flow over an accelerating permeable surface with heat source/sink, Internat. J. Engrg. Sci. 38 (2000) 1699–1712.
[22] S. Abel, K.K. Sujit, K.V. Prasad, Study of visco-elastic fluid flow and heat transfer over a stretching sheet with variable viscosity, Internat. J. Non-Linear Mech. 37 (2002) 81–88.
[23] T.C. Chiam, Heat transfer in a fluid with variable thermal conductivity over a linearly stretching sheet, Acta Mech. 129 (1998) 63–72.
[24] H.S. Takhar, M. Kumari, G. Nath, Buoyancy effects in boundary layers on a continuously moving vertical surface with a parallel free stream, Arch. Mech. 53 (2) (2001) 151–166.
[25] M. Acharya, L.P. Singh, G.C. Dash, Heat and mass transfer over an accelerating surface with heat source in presence of suction and blowing, Internat. J. Engrg. Sci. 37 (1999) 189–211.